Nuclear Magnetic Resonance Studies of the Solution Chemistry of Metal Complexes. I. Ligand-Exchange Kinetics from the Collapse of Metal–Proton Spin–Spin Coupling

Dallas L. Rabenstein

Contribution from the Department of Chemistry, The University of Alberta, Edmonton, Alberta, Canada. *Received August 27, 1970*

Abstract: The kinetics of the ligand-exchange reactions of the nitrilotriacetic acid (NTA) complex of lead have been measured from the extent of collapse of the lead-207–proton spin–spin coupling in the proton nmr spectrum of the complex. Rate constants were determined for the proton-assisted dissociation of the complex ($6.2 \pm 1.4 \times 10^4\ M^{-1}\ \mathrm{sec}^{-1}$) and for the displacement of the complexed NTA by completely ionized NTA ($6.6 \pm 1.4 \times 10^7\ M^{-1}\ \mathrm{sec}^{-1}$) and by monoprotonated NTA ($3.1 \pm 0.8 \times 10^3\ M^{-1}\ \mathrm{sec}^{-1}$). The rate constants were obtained by matching of experimental nmr spectra with theoretical nmr spectra which were calculated as a function of the lifetime of the complex using Bloch phenomenological equations modified to account for multisite exchange. The rate of displacement of complexed NTA by free NTA is significantly less for monoprotonated NTA than for completely ionized NTA, and the rate of the reaction of monoprotonated NTA with the aquated lead ion ($4.4 \pm 0.9 \times 10^6\ M^{-1}\ \mathrm{sec}^{-1}$) is less than that predicted for a mechanism in which the rate is controlled by water loss from the aquated lead ion ($\sim 6 \times 10^{10}\ M^{-1}\ \mathrm{sec}^{-1}$). Mechanisms are proposed for the reaction of monoprotonated NTA with the complex and with the aquated lead ion.

Nuclear magnetic resonance (nmr) spectroscopy is a powerful and direct tool for studying the solution chemistry of metal complexes; the nmr spectrum of the metal complex is sensitive to the chemical environment around the nuclei giving the nmr spectrum, thus providing information about the metal complex on the molecular level. Most reported nmr studies of metal complexes have involved proton nmr measurements on the complexed organic ligand(s) or on the solvent. These studies have provided solvation numbers for selected metal ions and have elucidated the stoichiometry, stability, and ligand-exchange kinetics for several metal complexes. Examples of applications of nmr to the study of these aspects of the chemistry of metal ions and metal complexes can be found in recent review articles.[1,2] The application of nmr to measuring ligand-exchange kinetics is the aspect of interest in the present paper.

A necessary condition for the nmr method for studying ligand-exchange kinetics to be applicable to a specific system is that the ligand exchange between nonequivalent environments of different chemical shifts.[3] The nmr line shapes for the magnetically active nuclei of the exchanging ligand depend on the dynamics of the exchange; this method is frequently referred to as the nmr line-broadening method. Exchange reactions that have been studied by the nmr line-broadening techniques are of the type

$$\mathrm{L^* + ML \rightleftharpoons ML^* + L}$$

where M is a diamagnetic or paramagnetic metal ion, L is the ligand, and the asterisk simply distinguishes between chemically identical ligand molecules.[4–8]

Another lifetime-dependent interaction sometimes observed in the proton nmr spectra of metal complexes of certain metal ions is spin–spin coupling between the isotopes of the metal ions whose nuclear spin quantum number I is $^1/_2$ and ligand protons.[8,9] Metal ions that have isotopes whose nuclear spin quantum number is $^1/_2$ include Pb, Cd, Hg, Pt, W, Fe, Rh, and Y. The metal–proton spin–spin coupling is observed only if the lifetime of the complex, τ_{ML}, is greater than $1/J_{\mathrm{MH}}$, where J_{MH} is the metal–proton spin–spin coupling constant.[10] At lifetimes less than $1/J_{\mathrm{MH}}$, the coupling collapses, with the degree of collapse depending on the lifetime. No quantitative studies of ligand-exchange kinetics based on the collapse of metal–proton spin–spin coupling have been reported, although the collapse has been observed in several systems and qualitative conclusions have been drawn from these observations.[11,12] The collapse of metal–proton spin–spin coupling has been used to study organometallic exchange reactions, *e.g.*, the intermolecular exchange of methyl groups in dimethylcadmium.[13,14]

In the present paper, the ligand-exchange kinetics of the nitrilotriacetic acid (NTA; $\mathrm{N(CH_2COOH)_3}$) complex of lead have been quantitatively studied by observing the collapse of the lead-207–proton spin–spin coupling for a range of solution conditions, including variations in ligand concentration and solution pH. NTA exchanges between the noncomplexed form and lead ions in three nuclear spin states, $+^1/_2$ and $-^1/_2$ for lead-207 and 0 for the other isotopes of lead, thereby

---

(1) T. R. Stengle and C. H. Langford, *Coord. Chem. Rev.*, **2**, 349 (1967).

(2) J. F. Hinton and E. S. Amis, *Chem. Rev.*, **67**, 369 (1967).

(3) J. A. Pople, W. G. Schneider, and H. J. Bernstein, "High-Resolution Nuclear Magnetic Resonance," McGraw-Hill, New York, N. Y., 1959, p 218.

(4) R. G. Pearson and R. D. Lanier, *J. Amer. Chem. Soc.*, **86**, 765 (1964).

(5) R. J. Kula and G. H. Reed, *Anal. Chem.*, **38**, 697 (1966).

(6) J. L. Sudmeier and C. N. Reilley, *Inorg. Chem.*, **5**, 1047 (1966).

(7) R. J. Kula and D. L. Rabenstein, *J. Amer. Chem. Soc.*, **89**, 552 (1967).

(8) D. L. Rabenstein and R. J. Kula, *ibid.*, **91**, 2492 (1969).

(9) R. J. Day and C. N. Reilley, *Anal. Chem.*, **36**, 1073 (1964).

(10) H. S. Gutowsky, D. W. McCall, and C. P. Slichter, *J. Chem. Phys.*, **21**, 279 (1953).

(11) P. D. Kaplan, P. Schmidt, and M. Orchin, *J. Amer. Chem. Soc.*, **91**, 85 (1969).

(12) T. A. Weil, P. J. Schmidt, and M. Orchin, *Inorg. Chem.*, **8**, 2138 (1969).

(13) N. S. Ham and T. Mole, *Progr. Nucl. Magn. Resonance Spectrosc.*, **4**, 91 (1969).

(14) W. Bremser, M. Winokur, and J. D. Roberts, *J. Amer. Chem. Soc.*, **92**, 1080 (1970).

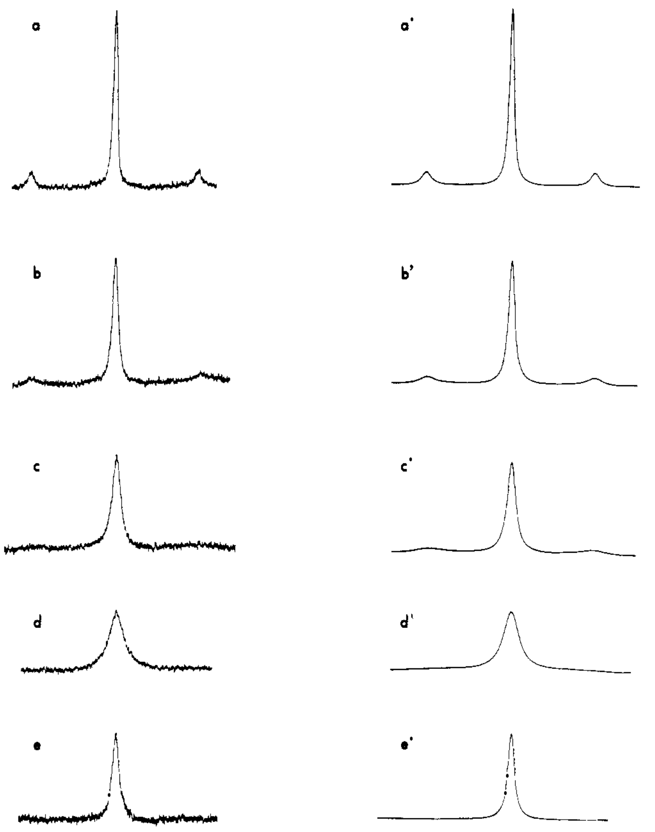

Figure 1. Experimental and calculated proton nmr spectra for $Pb(NTA)^-$ at pH 5.00 with varying concentrations of excess NTA. The concentrations of excess NTA are (a) 0.00 *M*, (b) 0.00082 *M*, (c) 0.0019 *M*, (d) 0.0056 *M*, and (e) 0.104 *M*. Calculated spectra were obtained using these concentrations of excess NTA and the rate constants listed in Table II for the Pb-NTA system.

providing a four-site random intermolecular exchange system. Exchange rate constants were obtained by matching theoretical spectra with experimental spectra; theoretical spectra were simulated using Bloch equations modified to account for multisite exchange. This study demonstrates that the collapse of metal-proton spin-spin coupling provides quantitative information on the dynamics of metal complexes in solution and extends the range of ligand-exchange reactions that can be studied by nmr methods.

Experimental Section

Chemicals. Nitrilotriacetic acid (K and K Laboratories, Inc.) and lead nitrate (Allied Chemical Co.) were used as received. Tetramethylammonium (TMA) nitrate was prepared by titration of a 25% aqueous solution of TMA hydroxide (Eastman Organic Chemicals) with HNO_3 to a neutral pH. The crystalline potassium salt of $Pb(NTA)^-$, KPbNTA, was prepared by a previously described procedure.[8]

pH Measurements. All pH measurements were made at 25° with an Orion Model 801 pH meter equipped with a standard glass electrode and a fiber-tip, saturated calomel reference electrode. Saturated potassium acid tartrate and 0.01 *M* sodium tetraborate buffers, pH 3.56 and 9.18, respectively, at 25°, were used to standardize the pH meter.

Nmr Measurements. Nmr spectra were obtained on a Varian A-56/60A high-resolution spectrometer at a probe temperature of 25 ± 1°. Spectra were recorded at sweep rates of 0.1 Hz/sec both for chemical shift measurements and line-shape measurements; sweep widths of 50 Hz were used. For line-shape measurements, each spectrum was recorded four or five times and the individual spectra were averaged.

The solutions used in the nmr studies were prepared in distilled water from the appropriate amounts of crystalline complex and H_3NTA. KOH was added to bring the solutions to the desired pH. TMA nitrate was added to each solution at a concentration of approximately 0.01 *M* as a reference compound for chemical shift measurements. The TMA resonance also was used as the criterion for acceptable magnetic field homogeneity. The proton nmr spectrum of TMA consists of three equally intense resonances, due to spin-spin coupling to nitrogen-14, separated by approximately 0.5 Hz. The magnetic field was adjusted until base-line resolution of the three peaks was achieved. Under these conditions, the magnetic field inhomogeneity contribution to resonance line widths is minimized. Chemical shifts are reported relative to the central resonance of the TMA triplet.

Results

Spectrum a in Figure 1 is the proton nmr spectrum of $Pb(NTA)^-$ in the absence of exchange on the nmr time scale, *i.e.*, when the lifetime of the complex, $\tau_{Pb(NTA)^-}$, is larger than $1/J_{Pb-H}$. The central resonance arises from the NTA protons in Pb(NTA) complexes of lead isotopes whose nuclear spin quantum number I is 0. The satellite resonances arise from the NTA protons of $Pb(NTA)^-$ complexes of lead-207 (natural abundance 22.6%) whose nuclear spin quantum number is $^1/_2$. J_{Pb-H} is small relative to the difference in resonance frequencies of the ligand protons and lead-207 so that the spin-spin coupling in $^{207}Pb(NTA)^-$ can be described as an A_6X situation.[15] Analysis of the spectrum yields 18.9 Hz for J_{Pb-H}. The central peak of the multiplet pattern is 39.8 Hz downfield from the central peak of the TMA triplet at 60 MHz.

The heteronuclear spin-spin coupling collapses at pH's less than 4.8, at pH's greater than 9.0, and when excess NTA is added to the solution; the extent of collapse depends markedly on solution pH and the concentration of excess NTA. The collapse of the coupling by excess NTA at pH 5.00 is shown in Figure 1. Qualitatively, the satellite resonances initially broaden and then merge with the central resonance while the central resonance broadens and then narrows as the concentration of excess NTA increases.

The extent of collapse of the coupling depends on $\tau_{Pb(NTA)}$; $\tau_{Pb(NTA)}$ is determined by the rates of the reactions causing dissociation of $Pb(NTA)^-$. Reactions 1-5 were considered to be the reactions that would result in dissociation of $Pb(NTA)^-$ for the solution conditions used in this study. Addition of excess

$$Pb(NTA)^- \underset{k_{-1}}{\overset{k_1}{\rightleftharpoons}} Pb^{2+} + NTA^{3-} \quad (1)$$

$$H^+ + Pb(NTA)^- \underset{k_{-2}}{\overset{k_2}{\rightleftharpoons}} Pb^{2+} + HNTA^{2-} \quad (2)$$

$$HNTA^{2-} + Pb(NTA^*)^- \overset{k_3}{\rightleftharpoons} HNTA^{*2-} + Pb(NTA)^- \quad (3)$$

$$NTA^{3-} + Pb(NTA^*)^- \overset{k_4}{\rightleftharpoons} NTA^{*3-} + Pb(NTA)^- \quad (4)$$

$$Pb^{*2+} + Pb(NTA)^- \overset{k_5}{\rightleftharpoons} Pb^*(NTA)^- + Pb^{2+} \quad (5)$$

$Pb(NO_3)_2$ to a solution of $Pb(NTA)^-$ until precipitation of a salt, presumably $Pb(PbNTA)_2$, occurred had no effect on the lead-proton spin-spin coupling, which indicates that for the solution conditions of this study the reaction represented by eq 5 does not contribute to the overall rate of dissociation on the nmr time

---

(15) Reference 3, p 480.

scale. Therefore, reaction 5 was not considered further in the analysis of the exchange kinetics of $Pb(NTA)^-$.

In each of the exchange reactions represented by eq 1–4 the NTA exchanges between the complexed and noncomplexed forms. The noncomplexed NTA is present as three species at the pH's used in this study, NTA^{3-}, $HNTA^{2-}$, and H_2NTA^-. A single, sharp resonance is observed for the carbon-bonded NTA protons in a solution containing only NTA at these pH's, indicating that exchange of the acidic protons between the differently protonated NTA species is rapid on the nmr time scale. Because proton exchange is rapid, the noncomplexed NTA can be treated as a single exchange site. The reactions represented by eq 1–4 thus provide a four-site, random, intermolecular exchange problem, the four sites being NTA in the noncomplexed form and $Pb(NTA)^-$ in three nuclear spin states, $+^1/_2$ and $-^1/_2$ for lead-207 and 0 for all other lead isotopes. The exchange problem is schematically illustrated in Figure 2.

The population of NTA in each of the four environments depends on the solution pH and on the amount of excess NTA added to the solution. The concentrations of the species present in each of the solutions studied were calculated by considering the following simultaneously occurring equilibria

$$NTA^{3-} + Pb^{2+} \rightleftharpoons Pb(NTA)^- \qquad (6)$$

$$K_f = [Pb(NTA)^-]/[Pb^{2+}][NTA^{3-}]$$

$$HNTA^{2-} \rightleftharpoons H^+ + NTA^{3-} \qquad (7)$$

$$K_3 = [H^+][NTA^{3-}]/[HNTA^{2-}]$$

$$H_2NTA^- \rightleftharpoons H^+ + HNTA^{2-} \qquad (8)$$

$$K_2 = [H^+][HNTA^{2-}]/[H_2NTA^-]$$

$K_f = 2.5 \times 10^{11}$, $K_2 = 3.2 \times 10^{-3}$, and $K_3 = 1.9 \times 10^{-10}$ (ref 8).

The rate constants for the reactions represented by eq 1–4 were evaluated from the lifetimes of NTA in each of the environments; the lifetimes were obtained by matching computer-simulated spectra with the experimental spectra. Spectra were simulated as a function of the lifetime of NTA in each of the environments using Bloch phenomenological equations modified to account for transfer of magnetization between the four environments by the chemical exchange reactions. Modified Bloch equations are valid for this case because the heteronuclear spin–spin coupling interaction is small compared to the difference in resonance frequencies of the coupled nuclei. The approach of McConnell and Meiboom was used to modify the Bloch equations for four-site exchange.[16,17] Spin–spin relaxation times, T_2, in the absence of exchange were calculated from the widths of the resonances measured under conditions of no exchange.[3]

Spectra were simulated by calculating the intensity of absorption at 0.05-Hz intervals over the frequency range 52.8–26.8 Hz downfield from TMA. The most convenient method of matching spectra was to compare the width at half height of the central peaks of the theoretical and experimental spectra. The individual rate constants were obtained from NTA lifetimes evaluated in this way for a range of solution conditions.

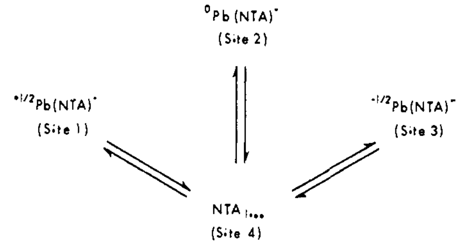

Figure 2. Schematic representation of the Pb–NTA exchange system.

The average lifetime of NTA in each of the four environments depends on the magnitude of the rate constants of the reactions represented by eq 1–4 and on the concentrations of reacting species. The rate of decrease in the concentration of $Pb(NTA)^-$ in each of its three environments is

$$-\frac{d[Pb(NTA)^-]}{dt} = k_1[Pb(NTA)^-] + k_2[H^+][Pb(NTA)^-] + k_3[HNTA^{2-}][Pb(NTA)^-] + k_4[NTA^{3-}][Pb(NTA)^-] \qquad (9)$$

Substitution of $\alpha_2[NTA_f]$ for $[HNTA^{2-}]$ and $\alpha_3[NTA_f]$ for $[NTA^{3-}]$ in eq 9, where α_2 and α_3 are calculated from the acid ionization equilibria,[18] followed by division by $[Pb(NTA)^-]$, leads to the following expression for the lifetime of $Pb(NTA)^-$

$$\frac{1}{\tau_{Pb(NTA)^-}} = k_1 + k_2[H^+] + (k_3\alpha_2 + k_4\alpha_3)[NTA_f] \qquad (10)$$

The lifetime of $Pb(NTA)^-$ is independent of its concentration; thus the lifetimes of $Pb(NTA)^-$ in its three different environments are equal. The rate of decrease in the concentration of NTA_f is

$$-\frac{d[NTA_f]}{dt} = k_{-1}[Pb^{2+}][NTA^{3-}] + k_{-2}[Pb^{2+}][HNTA^{2-}] + k_3[Pb(NTA)^-][HNTA^{2-}] + k_4[Pb(NTA)^-][NTA^{3-}] \qquad (11)$$

Substitution of $\alpha_2[NTA_f]$ for $[HNTA^{2-}]$ and $\alpha_3[NTA_f]$ for $[NTA^{3-}]$, followed by division by $[NTA_f]$, leads to the following expression for τ_{NTA_f}

$$\frac{1}{\tau_{NTA_f}} = k_{-1}[Pb^{2+}]\alpha_3 + k_{-2}[Pb^{2+}]\alpha_2 + (k_3\alpha_2 + k_4\alpha_3)[Pb(NTA)^-] \qquad (12)$$

In the pH region from 4.8 to 9.0, only the exchange reactions represented by eq 3 and 4 need to be considered; the presence of the heteronuclear spin–spin coupling in the spectrum of $Pb(NTA)^-$ in the absence of excess NTA indicates that the reactions represented by eq 1 and 2 are not contributing to chemical exchange on the nmr time scale in this pH region. In fact, the presence of the spin–spin coupling in this pH region indicates that rate constant k_1 cannot be determined by this method. The upper limit for k_1 in Table I was calculated by assuming that an increase of 0.2 Hz in the width at half height of the satellite peaks could be observed experimentally. The upper

---

(16) S. Meiboom, *J. Chem. Phys.*, **34**, 375 (1961).
(17) H. M. McConnell, *ibid.*, **28**, 430 (1958).
(18) H. A. Laitinen, "Chemical Analysis," McGraw-Hill, New York, N. Y., 1960, p 35.

Table I. Experimentally Determined Ligand-Exchange Rate Constants for NTA Complexes[a,b]

	Pb(NTA)	Cd(NTA)[c]	Zn(NTA)[c]
k_1, sec^{-1}	<0.6	<1	<1
k_{-1}, M^{-1} sec^{-1}	$<1.5 \times 10^{11}$	$<2.5 \times 10^{9}$	$<1.0 \times 10^{10}$
k_2, M^{-1} sec^{-1}	$6.2 \pm 1.4 \times 10^{4}$	$2.9 \pm 0.5 \times 10^{5}$	$1.8 \pm 0.8 \times 10^{5}$
k_{-2}, M^{-1} sec^{-1}	$4.4 \pm 0.9 \times 10^{6}$	$2.1 \pm 0.4 \times 10^{5}$	$5.1 \pm 1.0 \times 10^{5}$
k_{-2} (predicted), M^{-1} sec^{-1}	2.6×10^{10}	1.2×10^{10}	1.5×10^{9}
k_3, M^{-1} sec^{-1}	$3.1 \pm 0.8 \times 10^{3}$	$2.9 \pm 1.0 \times 10^{2}$	$5.3 \pm 0.6 \times 10^{2}$
k_4, M^{-1} sec^{-1}	$6.6 \pm 1.4 \times 10^{7}$	$1.8 \pm 0.3 \times 10^{7}$	$2.0 \pm 0.3 \times 10^{6}$

[a] 25°. [b] Error limits are obtained from the range of experimental values. [c] From ref 8.

limit for k_{-1} in Table I was calculated from the upper limit for k_1 using the relation $K_f = k_1/k_{-1}$. Rate constants k_2 and k_{-2} were determined from partially collapsed spectra at pH's less than 4.8, as described subsequently.

Table II. Nmr Kinetic Data for the Evaluation of k_3 and k_4[a,b]

		$W_{1/2}$, Hz	
pH	[NTA$_f$], M	Central peak	Satellite peaks
5.00	8.2×10^{-4}	0.80	1.76
5.00	1.3×10^{-3}	0.95	2.90
5.00	2.4×10^{-3}	1.26	*c*
5.00	3.4×10^{-3}	1.62	*c*
5.00	4.0×10^{-3}	1.73	*c*
5.00	4.5×10^{-3}	1.82	*c*
5.00	5.6×10^{-3}	2.04	*c*
5.00	6.2×10^{-3}	2.14	*c*
5.00	6.8×10^{-3}	2.24	*c*
5.00	2.9×10^{-2}	2.00	*c*
5.00	4.0×10^{-2}	1.59	*c*
5.00	5.0×10^{-2}	1.28	*c*
5.00	6.1×10^{-2}	1.19	*c*
6.00	1.1×10^{-4}	0.64	1.17
6.00	6.2×10^{-4}	1.16	*c*
6.00	1.1×10^{-3}	1.47	*c*
6.00	2.2×10^{-3}	2.46	*c*
6.00	2.7×10^{-3}	2.41	*c*
6.00	4.8×10^{-3}	2.28	*c*
6.00	6.9×10^{-3}	2.05	*c*
6.00	2.0×10^{-2}	1.13	*c*
7.00	6.2×10^{-4}	2.38	*c*
7.00	1.1×10^{-3}	2.22	*c*
7.00	1.6×10^{-3}	1.92	*c*
7.00	2.2×10^{-3}	1.63	*c*
7.00	3.2×10^{-3}	1.31	*c*
7.00	4.8×10^{-3}	0.96	*c*

[a] Pb(NTA)$^-$ is 0.10 M in each solution. [b] 25°. [c] Too broad to measure or not observable.

Neglecting the reactions represented by eq 1 and 2 in the pH region from pH 4.8 to 9.0, eq 10 and 12 become

$$1/\tau_{\mathrm{Pb(NTA)^-}} = k'[\mathrm{NTA_f}] \tag{13}$$

and

$$1/\tau_{\mathrm{NTA_f}} = k'[\mathrm{Pb(NTA)^-}] \tag{14}$$

where $k' = (k_3\alpha_2 + k_4\alpha_3)$. Experimental spectra were measured for a range of NTA$_f$ concentrations at each of three pH values (5.00, 6.00, and 7.00). k' was calculated from the values of the lifetimes that gave a simulated spectrum matching the experimental spectrum for each solution. The average values determined for k' are: pH 5.00, $k' = 4.41 \pm 0.6 \times 10^3$ M^{-1} sec^{-1}; pH 6.00, $k' = 1.50 \pm 0.4 \times 10^4$ M^{-1} sec^{-1}; pH 7.00, $k' = 1.24 \pm 0.4 \times 10^5$ M^{-1} sec^{-1}. k_3 and k_4 were evaluated graphically from these values by plotting k'/α_3 *vs.* α_2/α_3; the slope is k_3 and the α_2/α_3 intercept is k_4. The values obtained for k_3 and k_4 are listed in Table I. The experimental data are given in Table II.

Rate constant k_2 was obtained from the partial collapse of the coupling for Pb(NTA)$^-$ solutions at pH's less than pH 4.8. In this pH region, the reactions represented by eq 2, 3, and 4 contribute to the collapse; partial dissociation of Pb(NTA)$^-$ in this pH region gives sufficiently large concentrations of noncomplexed NTA that the reactions represented by eq 3 and 4 need to be considered. Experimental data are given in Table III. $\tau_{\mathrm{Pb(NTA)}}$ was evaluated for each solution by comparison of simulated and experimental spectra, and a value of k_2 was calculated for each solution using eq 15. The values determined pre-

$$1/\tau_{\mathrm{Pb(NTA)}} - (k_3\alpha_2 + k_4\alpha_3)[\mathrm{NTA_f}] = k_2[\mathrm{H^+}] \tag{15}$$

viously for k_3 and k_4 were used in the calculation of k_2; the concentration of NTA$_f$ in each solution was calculated by considering the equilibria represented by eq 12, 13, and 14. The average value obtained for k_2 is listed in Table I. k_{-2} was calculated from k_2 using the relation $k_{-2} = k_2K_3K_f$.

Table III. Nmr Kinetic Data for the Evaluation of k_2[a,b]

pH	$W_{1/2}$(satellite peaks), Hz
3.92	2.90
3.99	2.19
4.08	2.10
4.25	1.75
4.38	1.55
4.58	1.31

[a] Pb(NTA)$^-$ is 0.10 M in each solution. [b] 25°.

The simulated spectra shown in Figure 1 were calculated as described above using the concentrations of NTA$_f$ given for the experimental spectra in Figure 1 and the exchange rate constants listed in Table I.

Discussion

Spin-spin coupling of the type observed in the Pb-NTA system results from through-bond interactions.[19] NTA has four potential metal coordinating groups, three equivalent oxygen atoms, and one nitrogen atom, so that the lead-207 nuclei and the protons can couple *via* two different bonding systems, Pb-N-C-H and Pb-O-C-C-H. These two bonding systems differ in the donor atom coordinated to the lead-207 and in the number of intervening bonds between the lead-207 and the protons. Coupling through three bonds is

---

(19) Reference 3, p 185.

usually much larger than coupling through four bonds,[20] suggesting that the lead-207–proton coupling observed in the proton nmr spectrum of $Pb(NTA)^-$ occurs through the Pb–N–C–H bonds. This is supported by the finding that platinum–proton coupling through three bonds (Pt–N–C–H) is between 10 and 60 Hz, whereas platinum–proton coupling through four bonds is negligibly small.[21]

In solution, metal complexes of multidentate ligands like NTA undergo reactions that result in a change in the extent of coordination of the multidentate ligand to the metal (intramolecular reactions)[22–24] and reactions that result in complete dissociation of the multidentate ligand from the metal. Possible reactions for $Pb(NTA)^-$, assuming that there is octahedral coordination to lead, are shown in Figure 3. The lead–NTA bonds are constantly breaking and forming, resulting in interchange between the various species. The rates of interchange between the various species are rapid on the nmr time scale because only averaged resonances are observed for the NTA protons. Of the reactions shown in Figure 3, only the complete dissociation of NTA from lead causes the lead-207–proton spin–spin coupling to collapse. The intramolecular reactions involving the labile lead–oxygen bonds do not collapse the coupling because the bond system through which the coupling is transmitted is still intact. The coupling constant theoretically could change when the lead–oxygen bonds break if $J_{\text{Pb-H}}$ depends on the dihedral angle between the coupled nuclei because rotation about the C–N bond is now possible; however, this will not collapse the coupling. The intramolecular reactions involving the labile lead–nitrogen bond do not collapse the coupling because the nitrogen always rebonds to the same lead ion in the same spin state.[9] Thus, the lifetimes determined from the partially collapsed lead-207–proton spin–spin coupling are the average lifetimes of the $Pb(NTA)^-$ complex between events which lead to the complete dissociation of NTA from lead.

The lead-207–proton spin–spin coupling in $Pb(NTA)^-$ is pH dependent, partially collapsing at pH's less than 4.8 and at pH's greater than 9.0. Collapse occurs when τ_{PbL} is less than $1/J_{\text{Pb-H}}$ (0.053 sec for $Pb(NTA)^-$). Collapse at pH's less than 4.8 is due to the reactions represented by eq 2, 3, and 4. Calculations show that the collapse at pH's greater than 9.0 is due to reaction of the equilibrium amount of NTA^{3-} with $Pb(NTA)^-$, eq 4. For example, at pH 9.5, the concentration of NTA^{3-} in a 0.1 M solution of $Pb(NTA)^-$ is calculated to be 3.9×10^{-7} M using the equilibria represented by eq 6, 7, and 8. Considering only the reaction represented by eq 4, $\tau_{\text{Pb(NTA)}^-}$ is calculated to be 0.039 sec at pH 9.5, using the value given in Table I for k_4.

The rate constant for the reaction represented by eq 2 has been determined by Koryta to be 2.5×10^6 M^{-1} sec^{-1} using polarographic techniques,[25] compared to the value of $6.2 \pm 1.4 \times 10^4$ M^{-1} sec^{-1} determined in the present study. The fact that no observable collapse in the lead-207–proton coupling occurs down to pH 4.8 suggests that the value reported by Koryta is somewhat large. This can be seen from spectra calculated using Koryta's value of k_2. For example, at pH 5.0, Koryta's value of k_2 predicts a τ_{PbL} of 0.04 sec. Spectra calculated with a τ_{PbL} of 0.04 sec are collapsed, with the satellite peaks being barely detectable. However, in the experimental spectrum of $Pb(NTA)^-$ at pH 5.0, there is no observable collapse in the coupling (spectrum a, Figure 1).

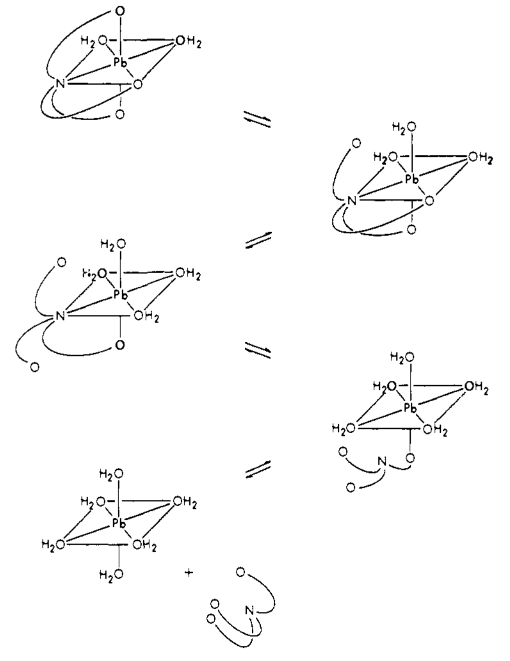

Figure 3. Reactions of $Pb(NTA)^-$ that lead to a change in the degree of coordination of NTA^{3-} to Pb^{2+} and to complete dissociation of NTA^{3-} from Pb^{2+}.

The mechanisms of multidentate ligand-exchange reactions have been the subject of much research.[5–8,22,23,26,27] Mechanisms have previously been proposed for exchange reactions analogous to the reactions represented by eq 1–4 in the Cd–NTA and Zn–NTA systems.[8] Comparison of the rate constants listed in Table I for the Pb–NTA, Cd–NTA, and Zn–NTA systems suggests that the mechanisms of the reactions in the Pb–NTA system are similar to the mechanisms in the Cd–NTA and Zn–NTA systems. The mechanisms discussed previously will not be discussed in detail here; however, several features supporting the conclusion that the mechanisms of the Pb–NTA reactions are similar to the mechanisms of the Cd–NTA and Zn–NTA reactions will be mentioned.

Rate constants k_3 and k_4 are both for second-order reactions involving the stepwise displacement of complexed NTA by free NTA. However, k_3 for the Pb–NTA system is $\sim 2 \times 10^4$ smaller than k_4, indicating that the rate-determining steps in the two reactions are different. These two reactions differ in the degree of protonation of the free NTA, $HNTA^{2-}$ for k_3 and NTA^{3-} for k_4. Two possible reaction mechanisms were proposed that account for the large decrease in the

---

(20) J. W. Emsley, J. Feeney, and L. H. Sutcliffe, "High Resolution Nuclear Magnetic Resonance Spectroscopy," Pergamon Press, New York, N. Y., 1965, p 174.

(21) L. E. Erickson, J. W. McDonald, J. K. Howie, and R. P. Clow, *J. Amer. Chem. Soc.*, **90**, 6371 (1968).

(22) D. W. Margerum, D. B. Rorabacher, and J. F. G. Clarke, Jr., *Inorg. Chem.*, **2**, 667 (1963).

(23) D. B. Rorabacher and D. W. Margerum, *ibid.*, **3**, 382 (1964).

(24) A. K. S. Ahmed and R. G. Wilkins, *J. Chem. Soc.*, 3700 (1959).

(25) J. Koryta, *Z. Elektrochem.*, **64**, 196 (1960).

(26) J. P. Jones and D. W. Margerum, *J. Amer. Chem. Soc.*, **92**, 470 (1970), and references cited therein.

(27) D. B. Rorabacher, T. S. Turan, J. A. Deferer, and W. G. Nickels, *Inorg. Chem.*, **8**, 1498 (1969).

displacement rate constants in the Cd–NTA and Zn–NTA systems upon protonation of the NTA.[8] (1) The reactive species is carboxylate-protonated $HNTA^{2-}$ while the major species present is nitrogen-protonated $HNTA^{2-}$ [8,28,29] (based on the relative basicities of carboxylate oxygen and nitrogen and statistically correcting for the number of carboxylate oxygens in NTA,[28] approximately one out of every 3×10^4 $HNTA^{2-}$ ions is carboxylate protonated). (2) The rate-determining step is the formation of the metal bond to the nitrogen of the reacting $HNTA^{2-}$ if the rate of transfer of the proton from the nitrogen of the reacting $HNTA^{2-}$ to another basic site is less than the rate of dissociation of the first-formed metal–carboxylate oxygen bond.[8] The difference between k_3 and k_4 for Pb–NTA is in good agreement with the predicted decrease if the carboxylate-protonated isomer of $HNTA^{2-}$ is the reactive species. Support for the second mechanism cannot be obtained from the rate constants for the Pb–NTA system because rate data for the dissociation of lead–carboxylate oxygen bonds are not available for comparison with the rate of proton migration from the nitrogen atom.

Rate constant k_{-2} is for the formation of $Pb(NTA)^-$ from aquated Pb^{2+} and $HNTA^{2-}$. The mechanism commonly proposed for the formation of metal complexes from aquated metal ions involves the loss of a water molecule from the aquated metal ion in an outer-sphere complex of metal ion and ligand, followed by bonding of the metal ion to the ligand at the vacated coordination site.[30] When steric and electrostatic effects are negligible, the rate-determining step in this mechanism is the rate of water loss from the metal ion. Steady-state approximations can be applied to the reaction sequence to express the observed formation rate constants, k_f, in terms of the individual steps. The result is that $k_f = K_{os}k^{-H_2O}$, where K_{os} is the outer-sphere association constant and k^{-H_2O} is the rate of water loss from the aquated metal ion. The rate of water loss from aquated Pb^{2+} has been reported to be comparable to that of Hg^{2+} ($\sim 2 \times 10^9$),[31] and K_{os} can be calculated using either the equations of Fuoss[32] or diffusion equations.[33] The predicted values of k_{-2} for the Pb–NTA, Cd–NTA, and Zn–NTA systems are listed in Table I. All of the observed values are much less than the predicted values, indicating that the rate-determining step in the reaction of aquated Pb^{2+}, Cd^{2+}, and Zn^{2+} with $HNTA^{2-}$ is not water loss from the aquated metal ions. The mechanisms proposed to account for the differences between the observed k_{-2}'s and the predicted k_{-2}'s in the Cd–NTA and Zn–NTA systems are analogous to those described above to account for the decrease in the rate of displacement upon protonation of the reacting NTA. The difference between the observed k_{-2} for the Pb–NTA system and the predicted k_{-2} is also in good agreement with the difference expected for the mechanism in which the reactive species is carboxylate-protonated $HNTA^{2-}$. Lack of data for the rate of dissociation of the lead–carboxylate oxygen bond prohibits drawing any conclusions about the second mechanism proposed above.

This study demonstrates that the dynamics of metal complexes in solution can be quantitatively measured from the extent of collapse of metal–proton spin–spin coupling. In the present study, this has been applied to symmetrical ligand exchange reactions of the type

$$L + ML^* \rightleftharpoons L^* + ML$$

The method should also be applicable to the study of the kinetics of any reaction which causes the complete dissociation of the complexed ligand. We are presently investigating its application to reactions of the type

$$X + ML \rightleftharpoons MX + L$$

where X and L are different ligands and

$$M + M^*L \rightleftharpoons M^* + ML$$

where M and M* are chemically identical metal ions.

Acknowledgment. This research was supported in part by a grant from the National Research Council of Canada.

---

(28) D. B. Rorabacher, Ph.D. Dissertation, Purdue University, Lafayette, Ind., 1963.

(29) J. C. Cassatt and R. G. Wilkins, *J. Amer. Chem. Soc.*, 90, 6045 (1968).

(30) M. Eigen and R. G. Wilkins, *Advan. Chem. Ser.*, No. **49**, 55 (1965).

(31) M. Eigen, *Pure Appl. Chem.*, **6**, 97 (1963).

(32) R. M. Fuoss, *J. Amer. Chem. Soc.*, **80**, 5059 (1958).

(33) M. Eigen, W. Kruse, G. Maass, and L. DeMaeyer, *Progr. React. Kinet.*, **2**, 287 (1964).